University of Texas at El Paso
ScholarWorks@UTEP

Open Access Theses & Dissertations

2022-12-01

Application Of FLO-SIC To f-Electron Systems: Sixth Row Elements And Ligated Molecules

Alexander Irun Johnson
University of Texas at El Paso

Follow this and additional works at: https://scholarworks.utep.edu/open_etd

 Part of the Physics Commons

Recommended Citation

Johnson, Alexander Irun, "Application Of FLO-SIC To f-Electron Systems: Sixth Row Elements And Ligated Molecules" (2022). *Open Access Theses & Dissertations*. 3690.
https://scholarworks.utep.edu/open_etd/3690

This is brought to you for free and open access by ScholarWorks@UTEP. It has been accepted for inclusion in Open Access Theses & Dissertations by an authorized administrator of ScholarWorks@UTEP. For more information, please contact lweber@utep.edu.

APPLICATION OF FLO-SIC TO f-ELECTRON SYSTEMS:

SIXTH ROW ELEMENTS AND LIGATED MOLECULES

ALEXANDER IRUN JOHNSON

Master's Program in Physics

APPROVED:

Mark Pederson, Ph.D, Chair

Tunna Baruah, Ph.D.

Koblar Alan Jackson, Ph.D.

Stephen L. Crites, Jr., Ph.D.
Dean of the Graduate School

©Copyright

by

Alexander Irun Johnson

2022

APPLICATION OF FLO-SIC TO f-ELECTRON SYSTEMS: SIXTH ROW ELEMENTS AND LIGATED MOLECULES

by

ALEXANDER IRUN JOHNSON, B.S.

THESIS

Presented to the Faculty of the Graduate School of

The University of Texas at El Paso

in Partial Fulfillment

of the Requirements

for the Degree of

MASTER OF SCIENCE

Department of Physics

THE UNIVERSITY OF TEXAS AT EL PASO

December 2022

Acknowledgements

I would like to acknowledge my advisor Dr. Mark Pederson, who made this work possible. I would also like to thank the rest of my thesis committee, Dr. Koblar Alan Jackson and Dr. Tunna Baruah for their generous discussions and guidance.

Abstract

Density functional theory - the most widely used theoretical method to study atoms, molecules, and solids - suffers from the well-known self-interaction error. A solution to the problem was suggested by Perdew and Zunger [1], who showed the self-interaction error can be removed with self-interaction correction. In 2014, Pederson showed a unitary transformation can be performed on the Kohn-Sham orbitals to generate Fermi-Löwdin orbitals which improve atomization energies, and avoid the computational costs of solving the localization equations.[2] This method is known as the Fermi-Löwdin Orbital Self-Interaction Correction (FLO-SIC). Until now, the FLO-SIC methodology has been used for atoms not containing f-electrons, because f-electrons were not implemented in the FLOSIC code, which is based on NRLMOL. This work presents an implementation of an f-electron capable NRLMOL including FLOSIC. Difficulties and strategies of FLOSIC with f-electrons are discussed, such as generating parameters known as Fermi-orbital descriptors used to define Fermi-Löwdin orbitals. Highest occupied molecular orbital energies are compared to experimental ionization potentials for several 6th row elements, which are particularly affected by self-interaction error. For some of the open shell elements, DFT predicts incorrect ground state valence configurations which can be recovered with FLOSIC. The results suggest that FLOSIC is a useful and efficient method to cure self-interaction error for systems containing f-electrons. Additionally, potential applications to molecular magnets are discussed, which are in dire need of an effective ab initio theory for accurate predictions.

Table of Contents

List of Tables

List of Figures

Chapter 1

Introduction

1.1 Molecular Magnets

Modern technology has taken a turn to harnessing quantum properties of new devices, and molecular magnets are a primary example. Practical applications are currently limited because their useful properties are often restricted to low temperatures and finding candidate molecular magnets is difficult. Lanthanide molecular magnets have seen a rise in popularity due to their large magnetic anisotropy barriers and large, localized spin states. [5] The first study on Lanthanide single molecule magnets (LnSMM) was published in 2003 [6]. The work showed that a Ln between two pthalocyanines $(LnPc_2)^-$ had ideal properties for use in molecular magnetism. The main argument for using rare earth elements in molecular magnets, spintronics, quantum computing, and other applications is that they exhibit high magnetic anisotropy energies due to the localized and shielded nature of the their valence f-electrons. This means the magnetic states of the systems tend to be longer lived and are more stable at higher temperatures. An example application of Ln molecular magnets is a single-molecule, two-qubit quantum gate (qugate) which contains two Ln atoms with states which allow for CNOT gate behavior, studied by Aguila *et al* in 2014.[7]

Most currently available molecular magnets only exhibit their ideal magnetic properties at temperatures much too cold for practical use, often requiring advanced cooling techniques such as liquid helium. If these magnets are to be used in products readily available to the general public, these properties must be brought to near room temperature conditions. A recent record breaking dilanthanide single molecule magnet was discovered which exploits divalent configurations of Ln, leading to a coupling of the 5d states of two Ln atoms. The f-

electron spins align parallel to the bonding orbitals, leading to a high spin state of S=15/2, and a coercivity greater than 14 T at 10K. The results suggest it is a powerful magnet at near liquid nitrogen temperatures. Lanthanide SMMs are a promising avenue to exploring potentially stable qubits at room temperatures. Although this thesis does not necessarily suggest ideal candidates for these uses, it lays a software foundation and tools that may be used and improved in future endeavors in FLO-SIC for f-electron systems.[8]

LnPc and $LnPc_2$ (Pc = phthalocyanine) are popular yet perhaps the simplest single molecule magnets, containing only one rare earth ion. As with most Ln molecular magnets, the nature of magnetism is in the unperturbed f-electrons while the d-electrons are credited for the bonding with ligands. DFT calculations performed on $LnPc_2$ by Candini *et al* [9] showed the f-states are below the Fermi-level as expected, but this result is attributed to the inclusion of a Hubbard U. The LDA+U approach introduces an extra layer of correlation for strongly correlated systems. The use of Hubbard U is a popular semi-empirical tool for correcting DFT, but it strays from the goal of an *ab initio* theory. It is useful to explore the obvious alternative of FLO-SIC, which is expected to stabilize the f-states similar to the Hubbard U, except it does not rely on semi-empirical methods.

Although the water saturated Cr^{3-} molecule does not include f-electrons, it is a significant challenge for density functional theory to describe that is expected to be improved with FLO-SIC.[10] The trianion system is known experimentally to be stable in water, however the orbitals resulting from a DFT calculation are delocalized and lead to an unstable trianion. FLO-SIC is known to stabilize anions, [11] and the effect is expected to improve the predicted stability Cr^{3-}. One challenge faced in studying the system with FLO-SIC is generating a starting point. A method of stabilizing the system by inclusion of nearby hydronium and subsequent removal of the additional proton are discussed in Section 4.2, and optimized starting structures are provided.

1.2 Rare Earth Elements

DFT is known to have difficulty for rare earth elements. The inclusion of f-electrons leads DFT to predict incorrect ground state electronic configurations, and often requires corrections such as a Hubbard U or hybrid functionals. [12] Although these methods can be useful, they are often used as semiempirical approaches, straying from the *ab initio* nature which makes them less appealing. The difficulties encountered with DFT for individual rare earth elements can lead to qualitatively incorrect results when allowed to interact with their environment, such as in calculations of LnSMMs which require a high degree of accuracy for predicting potential applications. With the flaws of standard DFT, which will be discussed next, the screening process for potential candidate LnSMM applications is restricted.

1.3 Kohn-Sham Density Functional Theory

The Schrodinger equation provides a template to describe any quantum mechanical system. However, when particles begin to interact, the equation becomes impractical to solve. In 1964, Hohenberg and Kohn showed that the total density can be used to calculate the ground state energy of any system given the exact exchange-correlation functional is known [13]. However, the exact functional is not known and must be approximated. The total energy is a function of the total density, ρ such that

$$E(\rho) = T(\rho) + U(\rho) + E_{XC}(\rho), \tag{1.1}$$

where T is the kinetic energy, U is the Coulomb or Hartree energy, and E_{XC} is the exchange-correlation energy. This energy expression obeys the variational principle such that the ground state energy is the lowest energy and is only described by the corresponding total density.

Kohn and Sham [14] further showed that the problem can be reduced from a many body interacting Hamiltonian to a non-interacting, one electron Schrödinger-like equation,

such that [14]

$$(\frac{-\hbar^2}{2m}\nabla^2 + \hat{V}_{Coulomb} + \hat{V}_{XC})\psi_i = \epsilon\psi_i. \tag{1.2}$$

where the first term is the kinetic energy operator and $\hat{V}_{Coulomb}$ is the Coulomb potential, and $\hat{V}_{XC}$) is the exchange-correlation functional. The Born-Oppenheimer approximation allows separation of nuclear and electronic wave functions such that nuclei are treated as point charges, so that the Coulomb energy is

$$\hat{E}_{Coul} = \sum_{A\neq B} \frac{Z_A Z_B}{|\vec{r}_A - \vec{r}_B|} + \sum_A \int \frac{Z_A \rho}{|\vec{r}_A - \vec{r'}|} dr + \frac{1}{2}\int\int \frac{\rho(\vec{r})\rho(\vec{r'})}{|\vec{r} - \vec{r'}|} d\vec{r} d\vec{r'}, \tag{1.3}$$

where A and B are nuclear indices.

Janak showed in 1978 that the orbital eigenvalues are equal to the derivative of the energy with respect to orbital occupation,

$$\frac{dE}{dn_i} = \epsilon_i. \tag{1.4}$$

Janak's theorem outlines a way of understanding fractionally occupied states that can occur for open shell systems in DFT.[15] The theorem can be verified that for any fractionally occupied system, the orbital eigenvalues of the fractionally occupied states must be equal. In cerium for example, local density approximation (LDA) predicts four occupied f-states that must have the same orbital energies.

The art of density functional theory is in improving the exchange-correlation functional to be more accurate. Many exchange-correlation functionals have been introduced, with increasing accuracy and computational expense. Jacob's ladder is a metaphor used to convey the relationship between the computational costs of calculations and chemical accuracy. For this work, results are focused on the lowest rung, using a local density approximation (LDA). The software also contains the Perdew-Burke-Ernzerhof (PBE) functional, which belongs to the second rung of Jacob's ladder as a generalized gradient approximation (GGA). More advanced functionals are available in the Public Release version of FLOSIC, but are not considered in this work.

1.4 Self-Interaction Error

Density functional theory suffers from a well known error, known as self-interaction error, and because the density does not distinguish between different electrons, the interactions of electrons with themselves is included in the Hamiltonian. The effects of this self-interaction are known, and must be carefully considered when using density functional theory in order to avoid incorrect conclusions about materials. In 1981, a solution to remove self-interaction error was proposed by Perdew and Zunger.[1]

1.4.1 Perdew-Zunger Self-Interaction Correction

In order to remove self-interaction error, Perdew and Zunger showed that for each electron, the self-interaction error contained in the exchange-correlation and Coulomb parts of the DFT energy could be removed on an orbital-by-orbital basis. [1] For each electron, Perdew-Zunger SIC removes the self-interaction, such that the electron electron potential is defined as

$$\hat{E}_{ee}^{SIC} = \hat{E}_{XC}^{DFT} - \sum_{i,\sigma}(\hat{E}_C(n_{i,\sigma}) + \hat{E}_{XC}(n_{i,\sigma}, 0)), \tag{1.5}$$

where $\hat{E}_{XC}^{DFT}$ is the standard DFT electron-electron interaction, $\hat{E}_C(n_{i,\sigma})$ is the self-Coulomb energy, and $\hat{E}_{XC}(n_{i,\sigma}, 0)$ is the self-exchange energy. The self-interaction terms depend on the orbital densities, $n_{i,\sigma}$. This is an effective method as it resolves the self-interaction error from DFT calculations in a systematical way, but it raises some issues. One is that the calculation is now orbital dependent and scales with the number of electrons. Another is the question of how to create physically accurate electronic orbitals from density functional theory calculations, as the canonical orbitals resulting from DFT are delocalized and do not give the minimal total energy, which is the objective of self consistent field calculations. Pederson, Ruszinsky and Perdew offered a solution to the latter.

1.4.2 Fermi-Löwdin Orbital Self Interaction Correction

In 2014, Pederson, Ruszinsky, and Perdew showed that a unitary transformation of Kohn-Sham orbitals can be performed to generate Fermi-Löwdin orbitals, which satisfy the requirements of Perdew-Zunger SIC by expressing the total density with localized orbitals.[2] First, Fermi orbitals are defined as

$$F_i = \frac{\sum_j \psi_j^*(a_i)\psi_j(r)}{\sqrt{\rho(a_i)}} \tag{1.6}$$

where a_i are Fermi orbital descriptors (FODs). The Fermi orbitals are then subjected to a Löwdin orthogonalization that guarantees the orbitals are orthonormal. It can be seen that the Fermi orbitals are implicitly localized at the position of the FODs, because the value of the square of the Fermi orbital at an FOD position is the total density at that point, thus the Fermi orbital is in some way localized near the FOD. After Löwdin orthogonalization, this is no longer true, but the orbital typically remains localized.

1.4.3 Fermi Orbital Descriptors

A difficult part of a FLOSIC calculation is generating FODs that lead to orthogonalizable Fermi-orbitals. A study has been conducted of methods created to generate FODs [16]. It is noted that FODs positions appear to have some physical meaning (e.g. FODs relax as points on spheres based on the principal quantum number of the electron they define. Bonds also tend to be represented by FODs located between atoms). More recently, a quick-FOD method was introduced, employing a pseudo-exchange repulsion to optimize starting positions for FODs.[17] Although these methods suffice for many systems, they have not been tested or used for f-electron systems. One of the big challenges tackled in this work is finding FODs for heavy atoms, which previously have not been explored.

1.4.4 Improvements

Several improvements are necessary in FLOSIC to improve the efficiency of calculations in general which will be addressed in this work, including: avoiding the Coulomb potential bottleneck, improving parallelization, rapidly evaluating FODs, generating good starting wavefunctions for FLOSIC calculations and modularity. The Coulomb bottleneck will be addressed by using the density matrix and analytic solution to Poisson's equation, which is algorithmically parallelizable to improve scaling. The same technique enables a modular tool which can be plugged into any existing DFT software to calculate SIC potentials, requiring minimal communication with the DFT code. A tool to generate unsymmetrized wavefunctions from symmetric DFT calculations is included, which allows selection of starting points for FLOSIC. A large scale application of the evaluation of FODs for a Cr^{3-} molecular magnet will be presented.

Chapter 2

NRLMOL and Implementation

NRLMOL was originally written with the intent to use s,p, and d orbitals, without regard to the use of f-electrons, in part because the computational expense of including f-states at the time was too great. As technology has evolved with Moore's law, we have an expanse of technology available, and it is no longer the expense of calculations that limit element calculations within standard DFT. Of course, scaling to large molecules make calculations more expensive, as well as addition of orbital dependence such as in FLO-SIC. In this chapter, I will discuss the necessary modifications to the standard NRLMOL code, a method to assist in scalability, as well as FOD considerations, particularly for f-electron elements, and selecting starting points.

2.1 Generalization to *f*-electrons

In order to generalize NRLMOL to include f-electrons and FLO-SIC, several considerations must be made. The primary functions in NRLMOL's workflow are to begin with a starting point, calculate density, calculate the DFT energy, and diagonalize the Hamiltonian to find new wave functions. The main modification is to allow the code to use f-type orbitals, which primarily requires allowing ℓ to increase from 2 to 3 and ensure all subroutines that know of the orbitals account for this change. Second, the basis set was expanded to include basis functions for f-states, as discussed in Section 3.1. Third, the standard Poisson subroutine, which calculates Coulomb interactions, is not easily modified to include f-electrons, and is also the bottleneck of FLOSIC calculations. An algorithmically parallelizable Poisson solver, discussed below, is implemented to attempt to resolve the bottleneck. The fourth

is to include the unitary transformation of the Kohn-Sham orbitals into FLOs, along with the calculation of SIC energies and addition to the potentials into the SCF hamiltonian. Previous work was done by Tunna Baruah and Mark Pederson to prepare parts of the code for f-electrons, particularly for relativity. [18]

The primary goal of this work is to allow for FLO-SIC calculations of f-electron elements, and therefore relativity and spin-orbit coupling were not included, however they are known to be important for f-electron element calculations, and should be included in later work.

2.1.1 Algorithmically Parallelizable Poisson Solver

Due to FLO-SIC being an orbital based method, calculations depend not only on the total density and resulting interactions, but also on the individual electronic orbitals and their interactions. As a result, the Coulomb potential calculation scales with the number of orbitals, and becomes the bottleneck of SIC calculations. In order to alleviate the scaling, efficient parallelization of the code becomes necessary. The standard method in NRLMOL to solve Poisson's equation relies on parallelizing over pairs of Gaussian orbitals. A new implementation, following the method described by Pederson [19], parallelizes over the basis set by summing one-dimensional Gaussian-quadratures in a way that reduces minimal storage from $O(N^2)$ to $O(N^{2/3})$. Furthermore, it could be used to parallelize over the mesh, though this has not been implemented. The method is implemented in a subroutine titled COUPOT1, and uses a DRVZPOT subroutine to calculate contributions to the Coulomb potential. The subroutine uses a previously written method, THCNDR, if there is no contribution of f-electrons. If f-electrons are included, a new subroutine ZPOT022821 is used which is generalized to include f-states. We expect this new method to scale best when there are a large number of basis functions (i.e. large number of atoms). This becomes particularly useful when f-electrons are involved. Due to the focus on atoms in this study, the scaling is not expected to show much improvement over the standard approach, and was not tested systematically. Computational efficiency was not explicitly studied during this project, however it would be useful to compare the efficiency of this new method to the

standard NRLMOL COUPOT1 subroutine. In order to verify numerical accuracy, energies for small molecules and atoms were compared to the public release version of FLOSIC. Energetics were numerically identical, and no deficiencies of the new method were found.

2.2 PZ SIC

The Perdew-Zunger self interaction correction was proposed in 1981, and is a logical solution to remove self-interaction error from DFT calculations that is exact in the limit of a one electron system. In order to remove the SIE, PZ-SIC becomes orbital dependent, calculating the self-Coulomb and self-exchange-correlation energies for each orbital as in eqn. 1.5 and removing the self-interaction energies from the DFT total energy. The SIC energies depend on the density of the orbitals, which makes the choice of orbitals important. Initially, canonical orbitals can be used, but do not satisfy the necessary physical constraints as they suffer from delocalization. The localization equations can be solved to obtain better orbitals, but scale on the order of $O(n^6)$.[20] I will discuss the use of canonical orbitals for Ln atoms as a proof of principle, and the more rigorous solution of using unitary invariance with Fermi-Löwdin orbitals to minimize the SIC total energy.

2.3 Spherical Approximation

In order to provide a proof of concept prior to full scale implementation of FLO-SIC, the Kohn-Sham orbitals resulting from self consistent density functional theory calculations were used in Eqn. 1.5 to give approximate self-interaction corrections, referred to here as ASIC. These orbitals are not localized, and adhere to the spherical symmetry of the atoms. This means the self interaction correction is underestimated in this approximation, and the orbitals do not satisfy the necessary requirements of Perdew-Zunger self-interaction correction (i.e. localization equations). However, they provide insight to the expected corrections from FLO-SIC calculations, and can be used for motivation. The method of

calculating spherical approximation SIC potentials is equivalent to FLO-SIC calculations, only with different orbitals. The ASIC results were used only to show progress and motivate further implementation of FLO-SIC.

2.4 FLO-SIC

FLO-SIC is implemented with Fermi-Löwdin orbitals. Fermi orbitals are defined by Eqn. 1.6. The current implementation of FLO-SIC in the f-electron code requires full occupations, and therefore was implemented such that occupations must be constrained beforehand in an EVALUES file, which is used to specify spin or occupation constraints and contains a breakdown of orbital energies throughout a calculation using NRLMOL. This differs from the available public release FLO-SIC[1] code which handles this implicitly. This is an adjustment that should eventually be addressed, and is being considered along with an initiative to simplify the many variations of UNRAVEL subroutines in NRLMOL which all have a similar objective to generate new wave functions, but are slightly modified for individual purposes such as using FLOs as opposed to Kohn-Sham orbitals.

2.4.1 Scissor Shift

As a temporary step to allow self consistent calculations, a scissor shift was implemented, adding the SIC energies to the LDA orbital energies. The scissor shift is defined as

$$P = \sum_i \Delta_i |\phi_i >< \phi_i|. \tag{2.1}$$

The shift matrix elements of the shift are written to a file and added to the DFT hamiltonian matrix prior to diagonalization. Including the FLO-SIC potential in the Hamiltonian enables self consistency. The scissor shift method is meant to be a temporary alternative to a more rigorous solution.

[1] available at https://github.com/FLOSIC

2.4.2 FOD forces

FODs must have a starting position to begin calculations. After a calculation reaches self consistency, these FODs are updated by calculating their forces according to the scheme provided by Pederson.[21] The public release version of FLO-SIC has forces implemented, and the subroutines were used in the current f-electron code. After calculating forces, a gradient descent method must be used to optimize FOD geometries. Both conjugate gradient and LBFGS methods are available in the f-electron code, however scaled-LBFGS is not yet implemented for f-electron atoms (Ba-Rn), and therefore should be used with caution. Further work may prove that scaling is necessary to improve the efficiency of calculations for f-electron atoms as this is the case for the lighter elements as shown by Withanage. [22] In the scaled-LBFGS scheme, the second derivative of the energy with respect to FOD positions are used to scale the gradients and FOD coordinates, which essentially makes the curvature of the energy surface roughly the same in all directions. The calculation of parameters used by the scaled-LBFGS scheme requires optimized FODs for the atoms, which are not yet available for f-electron containing atoms, and therefore this method is not possible until FODs are successfully optimized for heavy atoms using a different approach.

One difficulty that arises with f-electron calculations is the increased forces on the core FODs, which can lead to issues, such as crossing of 1s and 2s2p FODs, which result in confused gradient descent algorithms. A frozen 1s option has been included which allows the user to freeze the 1s FOD. Including an empty file named FREEZE1S in the calculation directory will enable this feature. This was used primarily when the 1s FOD moved significantly from the origin, often for open shell atoms. This issue will likely be resolved by a scaled force scheme, but a frozen 1s FOD is an appropriate fix and useful tool for the time being. An attempt at using effective potentials was implemented to normalize the FOD forces by a factor of $Z^{2(i/n-1)}$ where i is the principal quantum number and n is the maximum quantum number (for 6th row elements, n = 6). The effective potential is meant to mimic the second derivative of the forces, however the normalization did not

improve the optimization, often leading to linearly dependent FODs. Using a more robust scaling method, like the scaled-LBFGS method created by Withanage,[22] may improve optimization.

2.4.3 Starting Points

It is generally thought that FODs have some sort of physical interpretation, such that their location gives insight core and valence occupations, and to bond orders depending on the number of FODs along the axis of a bond. Tools have been developed, such as fodMC [16], to easily place FODs in a user configurable manner. There is evidence that the lowest energy solutions for organic molecules are found when FODs match the notion of a Lewis-like structure, where FODs may relax between bonded atoms, representing the bonded orbitals, and unpaired electrons being represented by FODs on the other side. Structural motifs such as tetrahedrons provide some insight on how to place initial FODs, as they are commonly seen in optimized FOD structures for lighter elements. However, it has yet to be shown for heavy elements how the FODs should be initially placed. The heavy elements have more complex electronic configurations, particular in the Ln series where f-electrons are considered valence, yet are localized and shielded from the environment. The current understanding of FODs is that they prefer to sit on spheres of differing radii based on the principal quantum number of the corresponding FLO. For organic molecules, is is simple to imagine that 1s FODs relax close to the nuclear position and the 2s and 2p FODs represent sp^3 hybrid orbitals, and relax to a tetrahedral motif around the nucleus. It gets more difficult when d-states become occupied and even further when f-electrons are introduced, and it is not straightforward to apply the current understanding of FODs to d- or f-states. In this work, a scheme to produce a database following a quasi-Monte Carlo approach is described and used to generate starting points for Rn, which are then optimized and modified to calculate 6th row elements.

Using the idea that FODs will relax onto spheres of radii based on quantum number, a random selection of symmetry groups is made to fill shells with FODs. The radius of

shells are estimated as the average radius of orbitals in an LDA calculation. The symmetry groups are sorted based on the number of points they can generate (e.g. x-axis symmetry will lead to reflection on the y-z plane to create 2 points, a tetrahedral symmetry will generate up to 24 points, etc.). The number of points in each shell is defined by principal number, and random groups which generate N points that are less than or equal to the number of FODs remaining to be filled for each shell are selected. Approximately 5000 potential FOD sets for each element from La (Z=57) to Rn (Z=86) were produced using this method to allow for exploration of many FOD structures. However, full self-consistent FLOSIC calculations of all FOD set candidates would be computationally expensive. An alternative method of selecting the optimal candidates from the many sets of FODs to perform FLOSIC calculations on is to calculate the overlap of the resulting Fermi orbitals, and choose the most orthogonal set by using some measure of orthogonality, such as the largest determinant of the overlap matrix, or the smallest sum of off-diagonal elements. The overlap of a pair of same spin Fermi orbitals is derived from Eqn. 1.6 as follows

$$< F_i|F_j >= \int \frac{\sum_\alpha \psi^*_\alpha(a_i)\psi_\alpha(\vec{r}) \sum_\beta \psi_\beta(a_j)\psi^*_\beta(\vec{r})}{\sqrt{\rho(a_i)\rho(a_j)}} d\vec{r}. \tag{2.2}$$

The integration over space is

$$\int \psi_\alpha(\vec{r})\psi_\beta(\vec{r})d\vec{r} = \delta_{\alpha,\beta}, \tag{2.3}$$

and the overlap matrix becomes

$$< F_i|F_j >= \frac{\sum_\alpha \psi^*_\alpha(a_i)\psi_\alpha(a_j)}{\sqrt{\rho(a_i)\rho(a_j)}}. \tag{2.4}$$

As hoped for by Pederson, the most loved orbitals are those that are most orthogonal.[21] Linearly dependent Fermi orbitals will not allow one to span the necessary space. We can define a measure of orthogonality for sets of Fermi orbitals as the minimum of S where

$$S = \sum_{i,j} | < F_i|F_j > |^2, \tag{2.5}$$

or use the maximum determinant or largest small eigenvalue. The FODMAT subroutine calculates the Fermi orbital overlap matrices and returns the measures of orthogonality. This method need not be rigorous, it is simply the tool to weed out candidates for good FOD starting points. Five of the most orthogonal sets of FODs for each atom were used for full SCF FLOSIC calculations, and the lowest energy set of FODs was selected to be optimized. The most success using this method was for Rn, whereas the other elements tested tended not to converge. The high failure rate of other elements (Z=57-85) is likely attributed to incorrect f-state occupations of the underlying density from DFT calculations, limiting the ability to find optimal starting FLOs. Despite the low success rate for heavy elements, this methodology allows for rapid sorting of FOD starting guesses and is not limited to individual elements. Similarly to the new method for calculating the Coulomb potential, the method is algorithmically parallelizable and therefore runtime decreases linearly with the number of processors.

2.4.4 Symmetric Starting Potentials

In addition to random FOD starting points, generating starting orbitals for FLOSIC calculations can be difficult for the 4f and 5d atoms. There are two methods to generate starting orbitals. The default is starting potentials, which create an initial Hamiltonian matrix to diagonalize and generate starting orbitals. The second method is to use orbitals from another calculation, typically DFT. It may be useful to use orbitals from DFT, but due to the incorrect occupations predicted by DFT for d- and f-shells, FLO-SIC can not always use DFT orbitals. One way of constraining DFT to agree with experimental configurations (and therefore make them more useful as FLO-SIC starting orbitals) is to generate correctly occupied orbitals by exploiting symmetry. In order to use these symmetrized orbitals, a method was implemented to generate the unsymmetrized wave functions from a symmetrized DFT calculation. It can be generalized for molecular calculations, though it is currently only implemented for single atom calculations. Using the unsymmetrized DFT wave functions allows us to pick the starting configuration for FLOSIC calculations

by giving the option to force occupation of symmetry representations in a DFT calculation. In essence, the method enables testing of customizable electronic configurations with FLOSIC to verify if FLOSIC improves the eigenvalue ordering of DFT. The method is unnecessary for cases where DFT is well behaved and gives the expected result (full shell and 6p atoms). Other cases for which DFT gives fractional occupation or disagrees with experimental configurations, this tool is useful. It could also be used to generate starting points for excited states and exciton calculations with FLO-SIC.

2.5 Hartree-Fock and Wave Function Overlap

In conjunction with work done by G. Flores, Hartree-Fock exchange and overlap of the multi-body wave functions from separate calculations were implemented in the code. The Hartree-Fock implementation mimics the algorithmically parallelizable Poisson solver, where only the individual orbitals are passed and the Hartree-Fock exchange energies are calculated.The tools allow for thorough analysis of DFT and FLO-SIC solutions. The Hartree-Fock implementation does not include self-consistency. The motivation for these tools is to develop a configuration interaction approach using DFT solutions. This work will not be discussed further in this thesis.

Chapter 3

Computational Details

All calculations in this work were conducted on UTEP's Jakar supercomputer, with the exception of the Cr^{3-} molecular magnet which required the larger compute power afforded by the National Energy Research Scientific Computing (NERSC) Center .

3.1 Basis Sets

The basis sets used by NRLMOL for f-electron containing elements were previously generated by Jens Kortus, using a code written by Dirk Porezag which generated optimized contracted coefficients. Four single Gaussian functions are used in addition to allow for improved descriptions of the f-electron orbitals. Developments are currently being made in finding minimal contracted basis functions using local optimization techniques, which takes advantage of the power of modern computers, and finds the best and minimal basis set for any given system. This work is currently being led by Sherab Dolma, and may be included in the future to further improve calculations including f-electrons, though its scope is intended for any DFT or FLO-SIC calculation.

3.2 Atomic Forces

Atomic forces in DFT calculations are identical to those previously available in NRLMOL, but now account for f-electron interactions. These forces were tested on a CH_4 using tetrahedral symmetry, and a minimal basis set with extra single Gaussian f basis functions. Using the format of (s, p, d, f) basis functions, the C atom in ISYMGEN has (2, 1, 0, 4)

functions, and H has (1, 0, 0, 4) functions in ISYMGEN. Using a bad basis set, such as this, is intentional to exaggerate the Pulay forces in the calculation, and verify the energy is still minimized. This test utilized an SCF convergence criteria of 10^{-6} Ha, and atomic force convergence criteria of 10^{-3} a.u. With the C atom at the origin, the H atoms were placed at a distance of 2.078 a.u. from the origin, and the first SCF LDA-exchange only energy was -39.426361 Ha. After optimization, the hydrogen were at a distance of 2.206 a.u. and an energy of -39.435461 Ha. The largest nuclear gradient at this optimized configuration was 1.42x10^{-5} a.u.

Similarly, Rn_2 was optimized to test atomic forces for heavy elements and an accurate description of the van der Waals bonding. The basis set used for Rn was the default of (9, 8, 6, 5) functions. The test utilized an SCF convergence criteria of 10^{-8} Ha, and atomic force convergence criteria of $1x10^{-4}$ a.u., with the PBE functional. The Rn atoms started at a separation of 10 a.u., without symmetry enforced, and an energy of -43741.23807308 Ha. The optimized separation was 9.4 a.u. with an energy of -43741.23808286 Ha. Both tests confirm that minimizing the energy is successful when f-electrons are included. The largest nuclear gradient at this optimized configuration was 1.69x10^{-5} a.u.

3.3 FLO-SIC

The general approach to optimizing FODs in FLO-SIC calculations involves minimizing both the energy and FOD forces. Typically for small molecules, an FOD force of 0.001 a.u. is reasonable. For the 6th row elements, forces on core FODs are much larger, some on the order of 0.1 a.u. Therefore, the criterion typically used for converged FLO-SIC calculations must be modified. Optimization of FODs for heavy atoms has proven to be a difficult problem for conjugate gradient, though it tended to perform better than LBFGS. Note that the FOD geometries may not be the optimal solutions for these atoms. The understanding of f-electrons in terms of FLO-SIC is still limited and must continue to be refined.

3.4 FLO-SIC with Symmetry

A recent development has been made in calculating SIC potentials for Fermi Löwdin orbitals using symmetry. In NRLMOL, this involves replacing several subroutines with a modular tool for symmetric FLO-SIC. The primary change is to call a subroutine called GETTTAT instead of APOTNL. GETTMAT calculates the total DFT energy, as well as the SIC energies for each inequivalent FLO. It utilizes SICHAM subroutine for these calculations. One of the most important changes is the replacement of calls to UNRAVEL with RxRAVEL, which is responsible for calculating wave functions in terms of the basis functions, and now RxRAVEL allows for symmetric FLOs. The MAPPER subroutine generates a minimal radial mesh to map symmetrically equivalent FLOs. Additionally, SIC potentials on mesh points where the FLO is zero are not necessary since the matrix elements involving the potential, V_i^{SIC}, are of the form $< \phi_j | V_i^{SIC} | \phi_i >$. Since FLOs are localized, it is possible to reduce the mesh when calculating SIC potentials for each FLO to only use grid points where FLOs are non-zero. This is accomplished by the CONDENSE subroutine. A FRMIDT file is used to define the inequivalent FODs, and a FRMORB file is generated which presents the entire set of FODs. An example FRMIDT for methane (CH_4) with tetrahedral symmetry is given in Appendix B.3.

3.5 Constraints Using Symmetry

For 6th row elements, it may be appropriate to use the same symmetry group as for LnPc structures as FOD structures could be used directly in the LnPc molecular magnet, though other groups (IH, OH, C3V, etc.) could be more useful for other applications. The symmetry group for LnPc has 16 operations, with 10 representations, and can be generated by the minimal transformations of x $\rightarrow$ y, x $\rightarrow$ -x, and z $\rightarrow$ -z.

Using Table 3.1, we can force DFT to occupy orbitals of our choosing. For example, for the Ce atom, we could occupy [Xe]$4f^1 5d^1 6s^2$ by selecting occupations for [Xe] with a

Table 3.1: List of representations, degeneracy, and states for the LnPc (Left), octahedral (middle), and icosohedral (right) symmetry groups. Representations with no s, p, d, or f states are indicated by *.

Rep.	Deg.	states
1	1	s,d
2	2	p,2f
3	1	d
4	1	p,f
5	2	d
6	1	f
7	1	d
8	*	*
9	1	f
10	*	*

Rep.	Deg.	states
1	1	s
2	3	p,f
3	3	d
4	1	f
5	2	d
6	3	f
7	*	*
8	*	*
9	*	*
10	*	*

Rep.	Deg.	states
1	1	s
2	3	p
3	5	d
4	3	f
5	4	f
6	*	*
7	*	*
8	*	*
9	*	*
10	*	*

valence configuration of representations 1 (s), 3 (d), and 6 (f) in the majority spin, and 1 (s) in the minority spin. For the open shell Ln atoms, this approach is used to generate starting wave functions for FLO-SIC calculations. This will be especially convenient when LnPc calculations with FLO-SIC are attempted.

Chapter 4

Molecular Magnets: Lanthanide Pthalocyanines and Cr^{3-}

The primary motivation of developing a code capable of FLOSIC with f-electron systems is to study molecular magnets. Ishikawa *et al* conducted the first study on LnSMM in 2003 using lanthanide Bis-phthalocyanines.[6] Since then, a plethora of LnSMM have been explored, yet the challenge to study these systems with computational techniques persists. [5] This serves as a primary motivation for this work, however FLOSIC calculations on LnSMM were not completed due to technical constraints which will be discussed in the next chapter, as the building blocks of individual elements must be tacked first. However, preparation for future FLOSIC caclulations is discussed here, using standard DFT to create starting molecular geometries. Progress towards studying a Cr^{3-} molecular magnet with FLOSIC is included. Although the trianionic system does not include rare earth elements, the affect of FLOSIC is expected be useful, and could late prove useful for finding solutions for LnSMM.

4.1 Preparation for LnPc

Fig. 4.1 displays the DFT optimized molecular geometry of BaPc. Standard DFT is unsuccessful at finding a stable electronic configuration for LnPc, which makes finding a molecular geometry impossible. Instead, BaPc was used to optimize atomic coordinates, such that Ba can be replaced with a lanthanide element when larger scale FLOSIC calculations are feasible. We believe LnPc will be the simplest rare earth molecular magnet, and

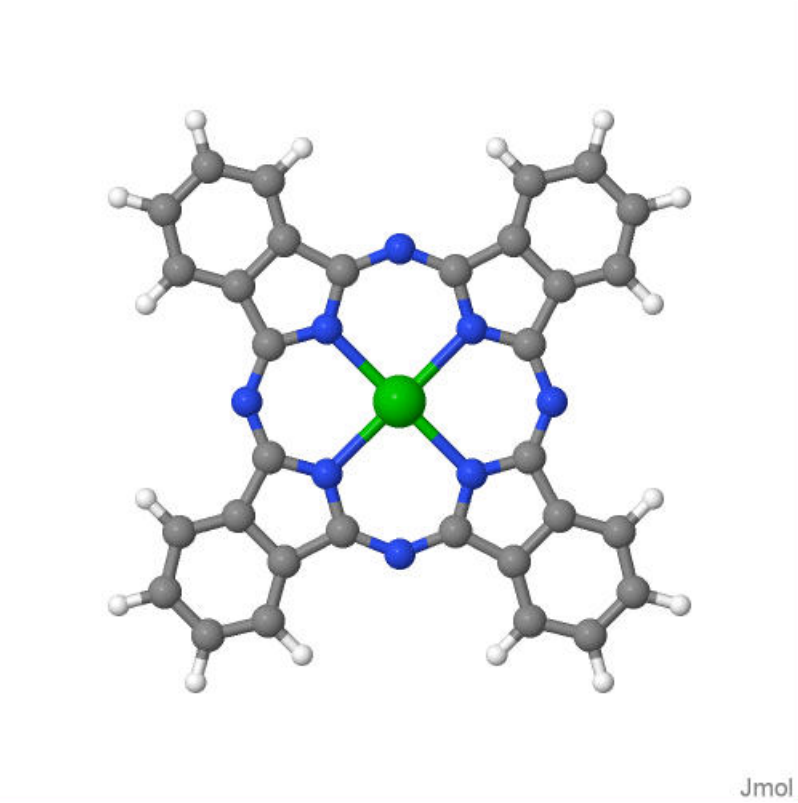

Figure 4.1: BaPc was used to generate starting points for LnPc calculations. Using rare earth elements (Eu, Gd) in place of Ba is not stable with standard DFT, but FLOSIC is expected to stabilize the electronic configuration for these systems. Jmol[4] was used to produce this image.

will be readily modified to $LnPc_2$ for comparison to the study by Ishikawa. [6]

4.2 Cr^{3-}

$Cr^{3+}(C_2O_4)_3^{2-}$, referenced here as Cr^{3-}, is a molecular magnet known experimentally to be stable in water. An optimized molecular geometry of the Cr^{3-}-in-water complex was provided by Mark Pederson. When studied with Density Functional Theory, the trianion molecular magnet becomes unstable and the charge becomes delocalized, resulting in an unphysical depiction of the molecular magnet.[23] In order to obtain a stable starting

potential for FLOSIC calculations, three additional hydrogen atoms were placed near the ends of the (C_2O_4) ligands, with an expectation that hydronium $(H_3O)^+$ molecules would form and contain the additional electrons on the trianion. The geometry was allowed to relax using the Perdew-Burke-Ernzerhof (PBE) generalized gradient approximation (GGA) until the largest nuclear gradient was below 0.01 a.u. As expected, hydroniums formed, but interestingly as part of a chain with two water molecules per hydronium. The additional protons successfuly stabilized the trianion. This leaves the system in a neutral charge state, so a pathway must be used to remove the proton after the initial state is generated, recovering the -3 charge state. This can be done by either changing the nuclear charge or by moving the proton from the molecular magnet to the edge of the water cluster. The optimized Cr^{3-} with hydronium system is shown in Fig. 4.2, with a hydronium and water chain highlighted.

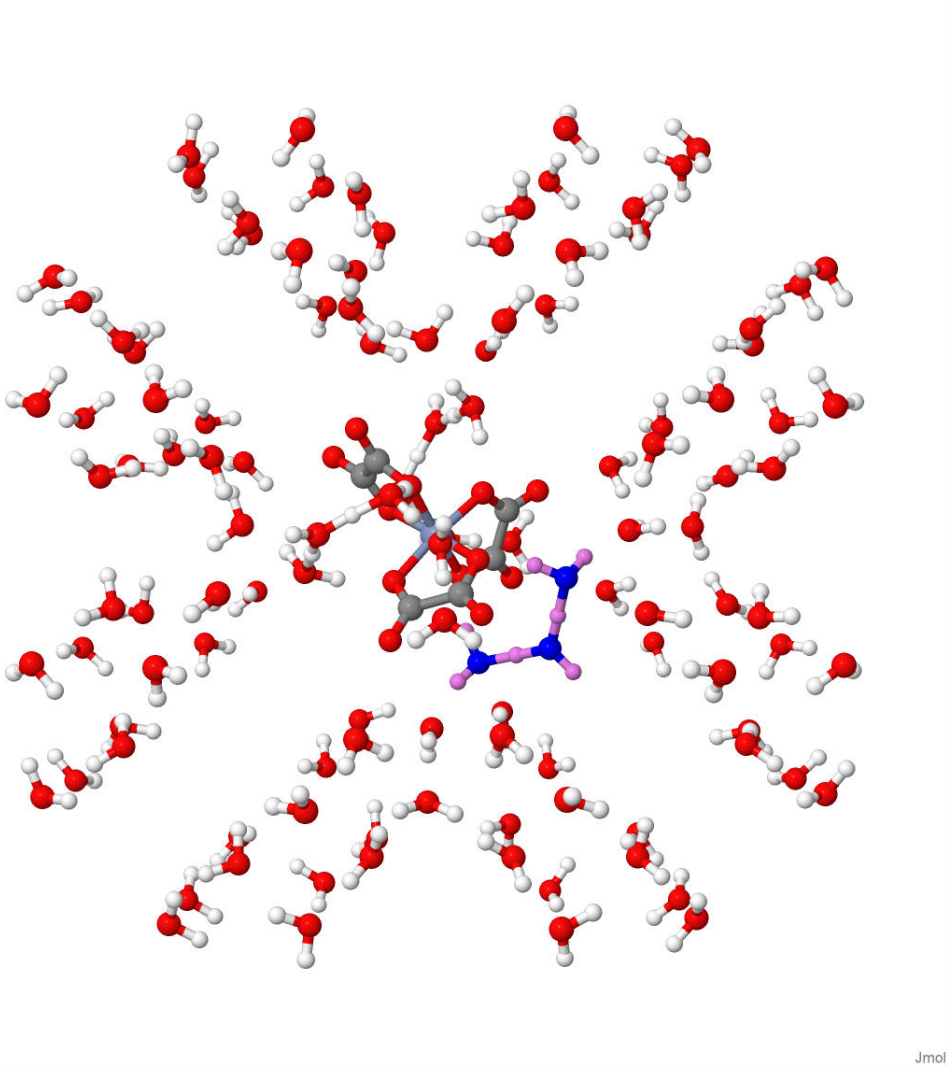

Figure 4.2: The $Cr^{3+}(C_2O_4)_3^{2-}$ molecular magnet in water $(H_2O)_{117}$, with three additional protons (H^+) included to stabilize the DFT trianion solution, serving as a starting density for FLOSIC. One of three hydronium and water chains is highlighted as blue oxygen and violet hydrogen. Jmol[4] was used to produce this image.

Chapter 5

6th Row Elements

5.1 Monte Carlo FOD generation

As shown in Tab. 5.1, the HOMO energies are improved by the inclusion of SIC when using the spherical approximation of the canonical orbitals. LDA HOMO energies consistently underestimate the ionization potential, and ASIC improves the HOMO energies towards experiment consistently for rare earth elements. These results were not intended to be significant, but rather only to provide motivation for continued implementation towards FLO-SIC and to test the numerics of the f-electron code.

Table 5.2 shows FLOSIC HOMO values. The same trend is seen as for the ASIC results. LDA HOMO values underestimate the experimental ionization potentials. FLOSIC improves the HOMO energy towards experiment. It is well known that FLOSIC correctly stabilizes anions and improves the description of ionization potentials. The results here suggest that the trend is maintained for f-electron systems. Additionally, DFT incorrectly predicts the ground state configurations of all rare earth elements except those with half occupied f-shells (Eu) or fully occupied f-shells (Yb and Lu). FLOSIC is expected to improve the ground state configurations, but due to difficulties in generating starting orbitals, this has not yet been realized in practice. The stability of these configurations throughout the self-consistent cycle is not consistent, so finding new FODs that lead to lower energy configurations may change this result in the future. The application of FLOSIC to 6th row elements is promising for larger f-electron containing systems.

The results do not include spin-orbit interactions or relativistic contributions, which are known to have large effects on heavy atoms due to the high angular momenta of f-electrons

Table 5.1: Spherical Approximation (ASIC) HOMO eigenvalues compared to standard LDA and experiment. Removing self-interaction from LDA improves the prediction of ionization potentials when comparing with HOMO energies. Experimental valence configurations are also provided, with a ✓next to the atoms where the LDA configuration agrees with experiment. *Experimental ionization potentials were obtained from [3]

Element	Exp. config.		LDA HOMO	ASIC HOMO	Exp. IP*
La	$5d^1 6s^2$		3.46	5.19	5.58
Ce	$4f^1 5d^1 6s^2$		3.55	5.30	5.54
Pr	$4f^3 6s^2$		3.32	5.02	5.47
Nd	$4f^4 6s^2$		3.35	5.06	5.53
Pm	$4f^5 6s^2$		3.37	5.10	5.58
Sm	$4f^6 6s^2$		3.39	5.14	5.64
Eu	$4f^7 6s^2$	✓	3.41	5.18	5.67
Gd	$4f^7 5d^1 6s^2$		1.86	4.37	6.15
Tb	$4f^9 6s^2$		3.52	5.35	5.86
Dy	$4f^{10} 6s^2$		3.56	5.42	5.94
Ho	$4f^{11} 6s^2$		3.61	5.49	6.02
Er	$4f^{12} 6s^2$		3.65	5.55	6.11
Tm	$4f^{13} 6s^2$		3.69	5.61	6.18
Yb	$4f^{14} 6s^2$	✓	3.68	5.63	6.25
Lu	$4f^{14} 5d^1 6s^2$	✓	3.03	6.49	5.43
MAE			2.43	0.61	

Table 5.2: HOMO energies of Eu, Yb, and Au-Rn. *Experimental ionization potentials were obtained from the CRC handbook [3]. *** At does not have an agreed upon experimental ionization potential energy.

element	LDA HOMO	FLOSIC HOMO	Exp. IP*
Eu	3.41	5.58	5.67
Yb	3.68	5.80	6.25
Au	4.66	7.68	9.23
Hg	4.66	7.65	10.44
Tl	2.95	5.67	6.11
Pb	4.20	7.01	7.42
Bi	5.39	8.95	7.29
Po	5.38	9.10	8.42
At	6.70	10.68	***
Rn	7.94	12.28	10.75
MAE	3.16	0.96	

and their localized nature. Spin-orbit coupling is enabled via a second-order perturbation [24], but is not currently implemented self-consistently and therefore would not affect the present results of orbital eigenvalues.

The optimized Rn FODs are shown in Fig. 5.2. The structure of the FODs follows the shell structure as assumed in the quasi-Monte Carlo methodology used to generate starting points, as discussed in Sec. 2.4.3. Using a cutoff of 10^{-4} for the smallest eigenvalue of the Löwdin overlap matrix to determine potential starting points, less than 8% of the 5000 potential FOD starting points for Rn were viable. Although attempts at using the same methodology for elements 57-85 were made, the success rate was much lower than that of Rn, and it proved to not be a viable method for generating FODs for all elements.

Instead, the resulting optimized FODs for Rn were used as a starting point for elements 57-85. FODs were removed from the Rn starting point to match the electronic configura-

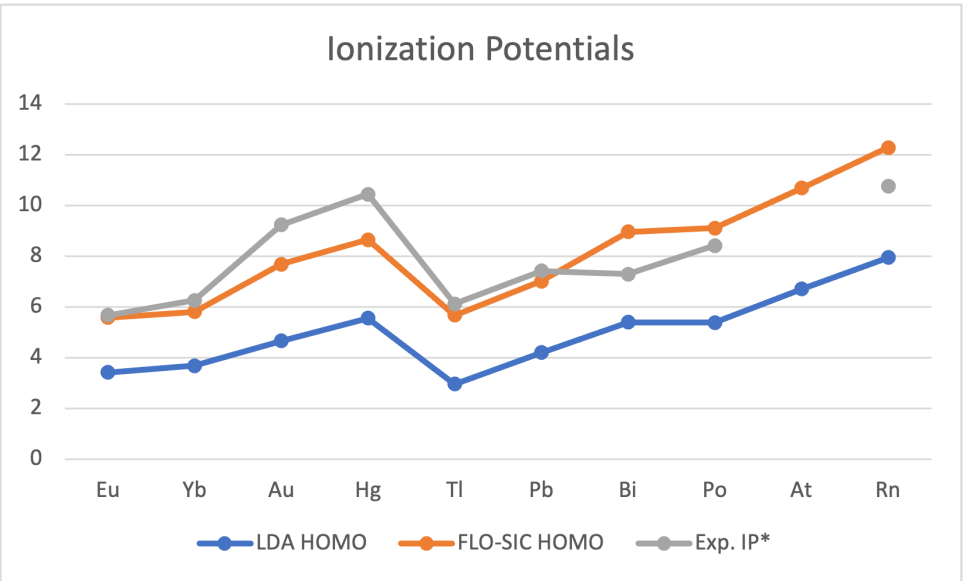

Figure 5.1: HOMO energies of Eu, Yb, and Au-Rn. *Experimental ionization potentials were obtained from the CRC handbook [3]. At does not have an agreed upon experimental ionization potential energy.

tion of the lighter elements, and the standard method of generating orbitals from starting potentials was used to start the calculations. This was successful for Eu, Yb and elements Hg-At. Note that FLOSIC was only successful for cases where the LDA configuration agreed with experiment (Eu and Yb), although the Lu calculation was unsuccessful. The resulting ionization potentials, estimated by HOMO energies, are shown in Table 5.2. The experimental result for At is not available, as the element is unstable and there is no agreed upon ionization potential for the element, and it is not included in the MAE. These were the only elements which did not result in linearly dependent FLOs using the Rn starting point. The FOD forces also varied, with Hg having the smallest max FOD force of 0.047 a.u., and Yb having the largest of 0.76 a.u. These forces are considered large for FLOSIC calculations, though this is expected for such heavy elements, and should be refined in the future.

It should be noted that starting points built upon different assumptions - such as mixing FODs of different principal quantum numbers or including differentiation of f- and d-FODs

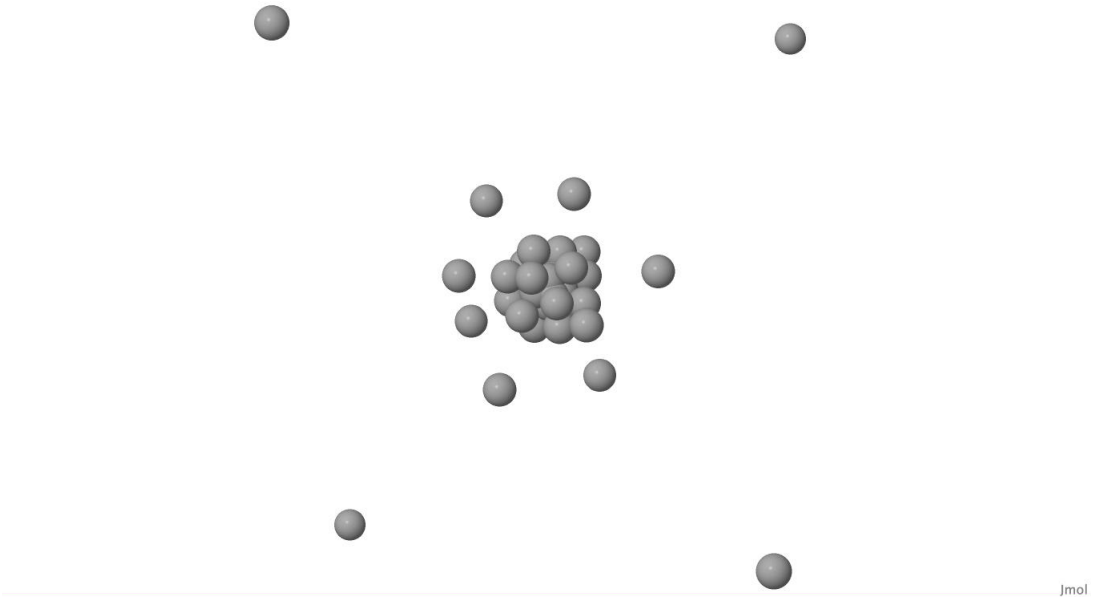

Figure 5.2: Optimized FODs for Rn. The FODs relaxed onto shells based on their principal quantum number. The outer tetrahedron is the 6s6p FODs. The next shell is the 5s5p5d, and inside that lies the 4s4p4d4f structure. The inner core (n=1-3) follows a similar structural ordering. Jmol[4] was used to produce this image.

to occupy different radii - may result in different FLOSIC solutions.

The full space of FODs should be explored to alleviate any concerns of bias, however this exercise would be expensive and further development to alleviate computational costs should be prioritized.

The FOD generator discussed in this section is a Monte Carlo style method, relying on random symmetry selection and rotations for each shell in order to generate starting points for FODs. It became apparent that starting from the pseudo-random starting FODs only proved viable for a subset of atoms. A more rigorous approach utilizing symmetry groups is presented in the next section.

5.2 C_{3v} Symmetric FODs

C_{3v} is a symmetry group of order 6 that is well suited for FODs because it allows for 1, 3, and 6 equivalent points. We maintain the assumption that FODs prefer to rest at radii defined by principal quantum number, n. Additionally, fully occupied s-shells need 1 FOD, p-shells require 3, d-shells require 5, and f-shells require 7. So for an n=1, there is 1s shell, and 1 FOD, which is assumed to be placed at the origin. n=2 is 2s2p, and requires 4 FODs. Typically, a 4 FOD shell is recognizable as a tetrahedron, as can be seen by examples such as Ne, or a CH4 molecule which forms sp3 hybrid orbitals. n=3 is 3s3p3d, or 9 FODs.

There is still discussion of the appropriate shape of FODs corresponding to d-orbitals. With our shared radii approach, and within the constraints of C_{3v}, we place the FODs on vertices of 3 triangles, rotated by 60 with respect to each other, with identical distance from the atom. For n=4, f-electrons are introduced, as 4s4p4d4f, and 16 FODs are required. We can utilize a subshell of 6 FODs, and supplement with a 9 FOD subshell similar to the n=3, and finished with a single FOD along the 111 axis. The n=5 shell of course can be generalized to g-orbitals, though no elements on the periodic table contain occupied g-orbitals. Therefore, shells up to a size of 16 are sufficient to define starting points for all elements, from hydrogen (Z=1) up to Og (Z=118)!

Utilizing C_{3v} symmetry, a FLOSIC solution of the heaviest element, Og. A new method, developed by Pederson *et al*, allows for removal of the FODs and corresponding FLOs or canonical orbitals from the solution to be used as starting orbitals for lighter elements.[25] Similar to the method discussed above, which involved removing FODs from a Rn solution, this method also removes FODs corresponding to the difference in number of electrons. Unlike the previous method, the standard starting potential of NRLMOL is not used. Instead, the FLOs corresponding to the removed FODs are also removed, and the resulting wave functions taken from the calculation of the heavier atom are used as the starting point for the lighter elements.

Chapter 6

Concluding Remarks

6.1 Significance of the Results

Self interaction error limits the capabilities of standard DFT methods from being applied accurately to rare earth systems. The current work has shown FLOSIC is capable of improving the description of f-electron systems using DFT. Although it is challenging to generate and optimize FOD structures, removing self-interaction error improves our ability to predict properties of heavy elements without the need for expensive wave function based methods. The new Poisson solver introduced in this thesis will help reduce the computational expense of FLOSIC calculations, and the methods described may assist in finding FOD solutions for more systems. FLO-SIC is a promising method for closing the gap between density functional theory and the more accurate (but more expensive) wave function based methods used today. f-electrons are particularly affected by self-interaction error as they are highly localized, and there is a clear benefit from making accurate predictions using FLOSIC. By improving our predictive abilities, we can advance applications that can exploit the unique properties afforded by rare earth molecular magnets. Although the methods applied fell short of applications to all of the rare earth elements or LnSMMs, it provides the software and technical background to expand rare earth studies with FLOSIC, as well as initial evidence that rare earth systems will benefit from FLOSIC. Already, new methods for finding starting FOD geometries, which rely on generating FODs and underlying electronic densities from simpler solutions, are proving that solutions can be found and that the capabilities resulting from this work can successfully be expanded. [25]

6.2 Future Work

The software developed in this work has many applications in the emerging fields of quantum computing, spintronics, and sensor applications using 6th row elements. Applying FLOSIC to well understood molecular magnets, such as $LnPc_2$ may provide further insight to the limitations and advantages of FLOSIC for rare earth systems. Additionally, computational expense is a drawback of FLOSIC. Further work to improve the calculation of the Coulomb potential and thorough investigation to reduce the time complexity may reduce the costs of future FLOSIC calculations.

Orbital eigenvalues were the main focus of comparison. A more complete comparison of FLOSIC for f-electron systems will improve our understanding and to help predict best use cases for the theory.

In parallel with this code, work is being performed on a periodic version of FLOSIC that can use similar methodologies to include f-electrons. The periodic version also includes an efficient numerical algorithm for single site Coulomb potentials that can be merged with the current work to improve atomic calculations.

FODs for LnPc systems have not yet been found, but a suggested method is to optimize the FODs of the ligand structure with a lighter element in place of the Ln element, such as Cu. Then, using the FODs of Rn, attempt to remove the necessary FODs from their corresponding shell to obtain the expected ground state configuration and replace the lighter element and corresponding FODs with the lanthanide atom. If the starting potential does not allow for FLOSIC to start (e.g. linearly dependent Fermi orbitals) a similar method to the Cr^{3-} molecular magnet may be useful. A nearby ion can be included to obtain a starting potential for the LnPc with DFT, and subsequently removed prior to the FLOSIC calculation.

References

[1] John P Perdew and Alex Zunger. Self-interaction correction to density-functional approximations for many-electron systems. *Physical Review B*, 23(10):5048, 1981.

[2] Mark R Pederson, Adrienn Ruzsinszky, and John P Perdew. Communication: Self-interaction correction with unitary invariance in density functional theory. *The Journal of Chemical Physics*, 140(12):121103, 2014.

[3] David R Lide et al. Crc handbook of chemistry and physics, 84th. *Electrochemical Series. CRC Press LLC*, 2004.

[4] Jmol: an open-source java viewer for chemical structures in 3d. http://www.jmol.org/.

[5] Daniel N Woodruff, Richard EP Winpenny, and Richard A Layfield. Lanthanide single-molecule magnets. *Chemical reviews*, 113(7):5110–5148, 2013.

[6] Naoto Ishikawa, Miki Sugita, Tadahiko Ishikawa, Shin-ya Koshihara, and Youkoh Kaizu. Lanthanide double-decker complexes functioning as magnets at the single-molecular level. *Journal of the American Chemical Society*, 125(29):8694–8695, 2003.

[7] David Aguilà, Leoní A Barrios, Verónica Velasco, Olivier Roubeau, Ana Repollés, Pablo J Alonso, Javier Sesé, Simon J Teat, Fernando Luis, and Guillem Aromí. Heterodimetallic [lnln] lanthanide complexes: toward a chemical design of two-qubit molecular spin quantum gates. *Journal of the American Chemical Society*, 136(40):14215–14222, 2014.

[8] Alexander I Johnson, Fhokrul Islam, Carlo M Canali, and Mark R Pederson. A multiferroic molecular magnetic qubit. *The Journal of chemical physics*, 151(17):174105, 2019. DOI: 10.1063/1.5127956.

[9] A Candini, D Klar, S Marocchi, V Corradini, Roberto Biagi, Valentina De Renzi, Umberto Del Pennino, F Troiani, V Bellini, S Klyatskaya, et al. Spin-communication channels between ln (iii) bis-phthalocyanines molecular nanomagnets and a magnetic substrate. *Scientific Reports*, 6(1):1–8, 2016.

[10] Der-You Kao and Shawn Domagal-Goldman. Magnetic anisotropy of a tri-anionic complex. In *APS March Meeting Abstracts*, volume 2019, pages A31–009, 2019.

[11] Jorge Vargas, Peter Ufondu, Tunna Baruah, Yoh Yamamoto, Koblar A Jackson, and Rajendra R Zope. Importance of self-interaction-error removal in density functional calculations on water cluster anions. *Physical Chemistry Chemical Physics*, 22(7):3789–3799, 2020.

[12] Mehmet Topsakal and RM Wentzcovitch. Accurate projected augmented wave (paw) datasets for rare-earth elements (RE= La–Lu). *Computational Materials Science*, 95:263–270, 2014.

[13] Pierre Hohenberg and Walter Kohn. Inhomogeneous electron gas. *Physical Review*, 136(3B):B864, 1964.

[14] Walter Kohn and Lu Jeu Sham. Self-consistent equations including exchange and correlation effects. *Physical Review*, 140(4A):A1133, 1965.

[15] James F Janak. Proof that $\frac{\partial E}{\partial n_i} = \varepsilon$ in density-functional theory. *Physical Review B*, 18(12):7165, 1978.

[16] Sebastian Schwalbe, Kai Trepte, Lenz Fiedler, Alex I Johnson, Jakob Kraus, Torsten Hahn, Juan E Peralta, Koblar A Jackson, and Jens Kortus. Interpretation and automatic generation of Fermi-orbital descriptors. *Journal of Computational Chemistry*, 2019. DOI: 10.1002/jcc.26062.

[17] Duyen B Nguyen, Mark R Pederson, John P Perdew, Koblar A Jackson, and Juan E Peralta. Initial Fermi orbital descriptors for flosic calculations: The quick-fod method. *Chemical Physics Letters*, 780:138952, 2021.

[18] Mark Pederson. Relativistic correction to the single-particle kinetic energy term. In *APS March Meeting Abstracts*, pages S32–004, 2005.

[19] Mark R Pederson. Communication: Practical and rigorous reduction of the many-electron quantum mechanical Coulomb problem to o (n2/3) storage. *The Journal of Chemical Physics*, 142(14):141102, 2015.

[20] Zeng-hui Yang, Mark R Pederson, and John P Perdew. Full self-consistency in the Fermi-orbital self-interaction correction. *Physical Review A*, 95(5):052505, 2017.

[21] Mark R Pederson. Fermi orbital derivatives in self-interaction corrected density functional theory: Applications to closed shell atoms. *The Journal of Chemical Physics*, 142(6):064112, 2015.

[22] Koblar A Jackson, Rajendra P Peralta, Juan Eand Joshi, Kushantha P Withanage, Kai Trepte, K Sharkas, and Alexander I Johnson. Towards efficient density functional theory calculations without self-interaction: The fermi-löwdin orbital self-interaction correction. *Journal of Physics: Conference Series*, 1290(1):012002, 2019. DOI: 10.1088/1742-6596/1290/1/012002.

[23] Der-You Kao and Shawn Domagal-Goldman. Magnetic anisotropy of a tri-anionic complex. In *APS March Meeting Abstracts*, volume 2019, pages A31–009, 2019.

[24] MR Pederson and SN Khanna. Magnetic anisotropy barrier for spin tunneling in $Mn_{12}O_{12}$ molecules. *Physical Review B*, 60(13):9566, 1999.

[25] MR Pederson, AI Johnson, KP Withanage, JGB Flores, Z Hooshmand, K Khandal, T Baruah, and KA Jackson. Downward quantum learning from element 118: Auto-

mated generation of Fermi-Löwdin orbitals for all atoms. [Manuscript submitted for publication].

Appendix A

New Coulomb Potential Solver

NRLMOL's existing COUPOT subroutine is responsible for calculating Coulomb potentials. It is the known bottleneck for FLOSIC calculations, because it is an orbital dependent theory and the potential for each orbital must be calculated separately. Using COUPOT to calculate Coulomb potentials for f-electrons would make the bottleneck even worse. Instead of attempting to improve COUPOT, a new method based on the methodology introduced by Pederson [19] was implemented, and is now the DRVZPOT subroutine. This method is expected to improve runtime for larger systems as it is algorithmically parallelizable, meaning the speedup will scale directly with the number of processors available, limited only by IO processes involved with increased number of processors. The algorithmic parallelization is easily understood as the calculation of Coulomb potential is not parallelized by mesh, but by basis set functions. With small systems, the improved parallelization is not very beneficial, and in fact is slower than the standard COUPOT subroutine. Large systems were not studied enough to determine whether the speedup is realizable. Additionally, the standard method of calculating the necessary components for the Coulomb potential is used when f-electron basis sets are not included, which is evident in the DRVZPOT subroutine. Parallelization was achieved using Message Passing Interface (MPI), and was tested on Jakar.

Appendix B

Input Files

The standard input files for NRLMOL are compatible with the f-electron code, with several updates. Some of the files follow the same format as the public FLOSIC code, in order to maintain interoperability for community adoption.

B.1 ISYMGEN

The ISYMGEN file must now include an entry for number of f-electron basis functions and supplementary f functions. Below is an example for Rn:

****

1 TOTAL NUMBER OF ATOM TYPES

86 86 ELECTRONIC AND NUCLEAR CHARGE

ALL ALL-ELECTRON ATOM TYPE

1 NUMBER OF ATOMS OF TYPE RAD

ALL-RAD001

EXTRABASIS CONTROLS USAGE OF SUPPLEMENTARY BASIS FUNCTIONS

25 NUMBER OF BARE GAUSSIANS

9 8 6 5 NUMBER OF S,P,D, F FUNCTIONS

0 0 1 0 SUPPLEMENTARY S,P,D,F FUNCTIONS

(Contracted coefficients and format omitted for brevity)

****

B.2 FODSETS

FOD overlap matrices for a large number of starting points can be calculated in older versions of the f-electron code, utilizing an FODSETS file. This feature was removed with the inclusion of symmetry, but could be re-implemented if needed in the future. An example for CH4 is provided

Filename: FODSETS

****

2 number of FOD sets (up to 100)

5 0 number of FODs (spin up, spin down)

0.0 0.0 0.0

1.0 1.0 1.0

-1.0 -1.0 1.0

-1.0 1.0 -1.0

1.0 -1.0 -1.0

5 0 number of FODs (spin up, spin down)

0.0 0.0 0.0

1.2 1.2 1.2

-1.2 -1.2 1.2

-1.2 1.2 -1.2

1.2 -1.2 -1.2

****

B.3 FRMIDT

The FRMIDT file is used for symmetric FOD structures, and includes the inequivalent FOD points. Below is an example for $CH4_4$, using tetrahedral (TD) symmetry.

Filename: FRMIDT

****

2 5 0 0 number of up inequivalent, up equivalent, down inequivalent, down equivalent

0.0 0.0 0.0 1 1 (x y z coordinates, FOD ID, equivalent FOD IDs)

1.2 1.2 1.2 4 2 3 4 5 (x y z coordinates, FOD ID, equivalent FOD IDs)

****

B.4 MODE

The MODE file contains an integer used to initiate Hartree Fock calculations. The purpose for this file is work done by G. Flores, and is not discussed here. The options are:

1 = do not use the Hartree Fock code

2 = collect Hartree Fock energy and wave functions

3 = calculate overlaps of Hartree Fock wave functions

Option 1 is used throughout this work.

Filename: MODE

****

1

modes: 1=normal,2=collect,3=overlaps

****

Appendix C

Software availability

The code used for the calculations reported here is currently in a private GitHub repository. Please reach out to Alexander Johnson or Mark Pederson to obtain access.

Curriculum Vita

Alexander Johnson earned his bachelor's degree from Central Michigan University in 2020. He grew interested in density functional theory and self-interaction correction during the course of his undergraduate career. A collaboration on the Fe_3 molecular magnet motivated work towards improving DFT for controlling molecular magnets. He moved to the University of El Paso to join the Molecular Magnetism and Quantum Theory Lab to pursue a master's degree in physics.